Materials Research Proceedings 35 (2023) 62-69 https://doi.org/10.21741/9781644902714-8

Modelling the laser overageing treatment of a 6xxx Al alloy by means of physical simulation tests

Antonio Piccininni[1,a*], Pasquale Guglielmi[1,b] , Angela Cusanno[1,c] and Gianfranco Palumbo[1,d]

[1] Department of Mechanical Engineering, Mathematics and Management, Politecnico di Bari, 70126, Italy

[a]antonio.piccininni@poliba.it, [b]pasquale.guglielmi@poliba.it, [c]angela.cusanno@poliba.it, [d]gianfranco.palumbo@poliba.it

Keywords: Laser Heat Treatment, Aluminium Alloys, Hardness

Abstract. The local modification of the material properties is a promising strategy to broaden the range of applications for Aluminum (Al) alloys, since excessive thinning are avoided, and sound parts obtained. For example, by means of laser heating, the strain behaviour of age hardenable Al alloys can be locally affected to enhance the formability at room temperature. But predicting the properties modification (occurrence of overageing/solutioning) due to the local heating still needs investigations. In this work, short-term heat treatments on AA6063-T6 samples were conducted using the Gleeble system (able to subject the material to high heating rates combined with large temperature gradients). Wide ranges of temperature and time were thus explored, and the change of mechanical properties assessed by hardness tests. Experimental data were used to create a model and thus define the heating parameters able to bring the material to the overaged state or, alternatively, to the fully solutioned one.

Introduction

The reduction of fuel consumption in the transportation sector is becoming one of the most urgent issues to be tackled [1]. The reduction of sprung/unsprung masses in vehicles [2] is one of the most direct solutions to reduce pollution trying, at the same time, to meet the standards of passengers' comfort and safety [3]. In light of this, the scientific research has focused the attention on the definition of new products able to combine limited weight, good level of strength, and high standard of safety. Aluminum (Al) and its alloys are regarded as ideal candidates to match all the mentioned requirements: in particular, especially for the automotive sector, the adoption of tubular structural parts has shown several advantages since they can combine the necessary stiffness without excessively increasing the vehicle's weight. Despite all the advantages in terms of limited density and high strength-to-weight ratio, the adoption of Al alloys for structural and complex components is partially hindered by the low formability at room temperature [4]. Therefore, innovative manufacturing solutions have been investigated. Among the others, the approach based on the local modification of the material properties by means of a short-term heat treatment has demonstrated huge potentialities [5]: in such a way, the properly optimized alternation of strength and ductility improves the alloy formability at room temperature. Moreover, being the forming operations carried out at room temperature, costs related to the equipment are sensibly lowered. Literature confirms the effectiveness of the mentioned approach especially when applied to sheet metal parts [6,7], whereas only few examples deal with the possibility to apply a local modification to tubular components [8]. Nevertheless, it is reported that laser treatments, when applied to AA6063-T6 tubular samples, influences the deformation behaviour when the tube is deformed by the action of an elastomer [9]. Nevertheless, the question is not trivial: according to the precipitation kinetics in Al-Mg-Si alloys [10], if subjecting the material in the T6 "peak hardening" state to a heat treatment, two different outcomes can be obtained: (i) a temporary alteration of the

Materials Research Proceedings 35 (2023) 62-69 https://doi.org/10.21741/9781644902714-8

properties brining the alloy to the fully solutioned condition which is characterized by higher formability but highly metastable (if kept at room temperature, it evolves due to the triggering of the natural ageing) or (ii) a permanent alteration, i.e. the overaged condition, which is characterized by an improvement of the material formability that is stable with time [11]. Given that, the gap still to be bridged is the definition of an accurate methodology that is able to predict the effect of short-term heating on the properties distribution.

Therefore, in the present work, a methodology based on the physical simulation is proposed to numerically predict the occurrence of the overaged state in a AA6063-T6 tubular component locally heated by means of a laser heat treatment. Thanks to a reduced number of tests using the Gleeble system, the combination of temperature and time able to determine the overaged or the fully solutioned state could be determined by hardness measurements along the heat-treated samples. In particular, hardness values were then fitted by a logistic function that was subsequently implemented in a python script. Laser heating of the tubular part (initially supposed in the T6 condition) was simulated by means of the Finite Element (FE) code Abaqus and results post-processed by means of the above-mentioned script to numerically predict the final distribution of hardness over the treated area. Numerical predictions were eventually validated by experimental laser heating tests. The proposed results can be regarded as preliminary steps toward a flexible and on-demand manufacturing approach of tubular components (starting from high-strength but difficult-to-form materials of automotive interest) with tailored behaviour coming from local features.

Calibration of the overageing heat treatment

Specimens were extracted from AA6063 tubular samples (200 mm long) in the T6 condition and heat treated using the physical simulator Gleeble 3180. Figure 1a shows a detailed view of the specimen positioned in the test chamber and clamped, at its end, by means of two cooled grips. The specimens is heated by Joule effect due to the current flow which is continuously modulated according to the temperature data acquired by a thermocouple (TC2) welded in the middle part of the specimen (black spot in Figure 1a). The performed heat treatment was composed of: (i) a heating step with a rate of 400°C/s (thus approximately reproducing the passage of a laser), (iii) a soaking step during with the test temperature was kept in the region of the TC2 and (iii) a final cooling step by blowing air inside the test chamber. Being the grips cooled, the sample experienced a temperature decrease moving from the middle position (where TC2 was positioned) toward the two ends: a parabolic distribution was supposed, which determined several and simultaneous heat treatments within the same tests. Thanks to the welding of the four thermocouples and assuming that the temperature distribution was symmetric with respect to the TC2 position, the parabolic trend could be reconstructed based on 7 points as shown in Figure 1b (plotted curve refers to the test temperature at 350°C for 5 seconds; filled markers refer to the acquisition from the TC).R

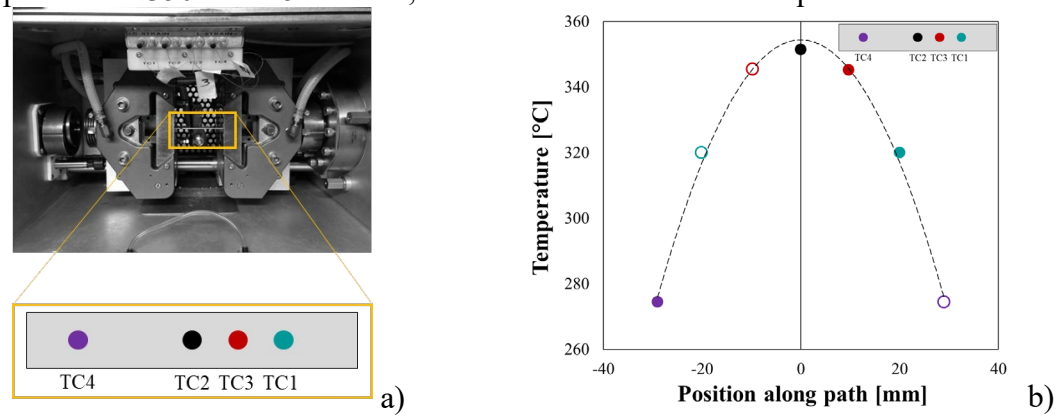

Figure 1 Set-up for the preliminary characterization: (a) detail of the Gleeble test chamber, (b) parabolic distribution of properties for the test temperature of 350°C

Materials Research Proceedings 35 (2023) 62-69 https://doi.org/10.21741/9781644902714-8

Once cooled down to room temperature, specimens were subjected to hardness measurements (using the Qness micro hardness tester Q10 A+, setting a load of 200 g and a dwell time of 15 s) along the longitudinal direction and at regular interval of time to evaluate the achieved overaged condition or, alternatively, the fully solutioned one.

Experimental laser heating tests

Laser heating on tubular components were carried out using a 2.5 kW CO_2 laser head (A in Figure 2a) equipped with a Diffractive Optical Element (DOE) to obtain a top-hat energy distribution. A preliminary test was carried on a 200 mm long AA6063 tube (external diameter of 40 mm, average thickness of 1.9 mm) initially in the T6 condition: the tube (B in Figure 2a) was preliminarily sprayed with a black paint for high temperature (to increase the absorption of the laser radiation), positioned on a designed fixture (C in Figure 2a) and laser heated under a constant power of 600 W (square laser spot of 10 mm) for 5 seconds at a distance of 63 mm from the one of its ends. The temperature evolution was monitored by a wire thermocouple (D in Figure 2a) welded on the inner surface of the tube in correspondence of the laser spot's center (the correspondent temperature-time curve is plotted in Figure 2b). Additional laser heating tests were finally carried out to validate the numerical predictions.

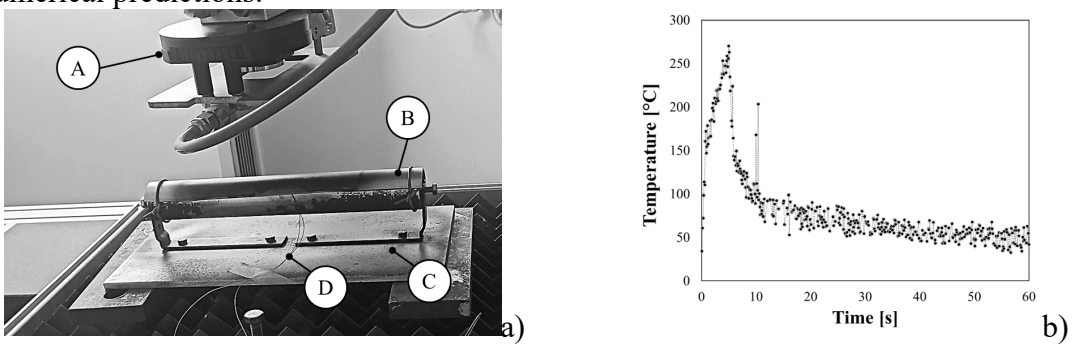

Figure 2 Laser heating tests: (a) experimental set-up; (b) temperature acquired from the thermocouple

Numerical simulation of the laser heating

The tube laser heating on a tubular component was simulated with the FE commercial code Abaqus/CAE. The tube was modelled as a deformable body and meshed with 46400 DC3D8 8-node solid elements (average size of 1 mm). The heat treatment of the tubular specimens was simulated solving the pure thermal transient problem (using the implicit solver): preliminary simulations were run to calibrate the unknown thermal boundary conditions – i.e. the quantity of absorbed radiation by the material and the heat transfer coefficient between the tube and the surrounding environment – by minimizing the difference between the experimental temperature acquisition from the thermocouple (as shown in Figure 2b, it was welded to the underside of the sample) and the numerical temperature curve extracted from the node at the same location. Once calibrated the thermal model, subsequent numerical simulations, keeping the same heating strategy (laser spot at 63 mm from the tube's end), were run changing the laser power and the heating time over three levels (600 W, 800 W, 1000 W for the laser power and 5 s, 10 s and 15 s for the heating time). Results from the numerical simulations were post-processed by means of a python script to predict the final hardness distribution.

Results from the calibration of the overageing heat treatment

The first heating tests were carried out setting the temperature to 450°C and the soaking time to 2 s. Local temperature evolutions could be extracted (see Figure 3a): during the soaking time the parabolic distribution embraced temperatures between 450°C (at the TC2 location) and 400°C (at the TC4 location). The results of the hardness measurement, shown in Figure 3b, demonstrate that all the specimen's points heated at temperatures included in the parabolic distribution were brought

Materials Research Proceedings 35 (2023) 62-69 https://doi.org/10.21741/9781644902714-8

to the fully solutioned state: the hardness, in fact, evolved (natural ageing) from an average value of 50 HV (1 h after the heat treatment) up to around 80 HV (one week after).

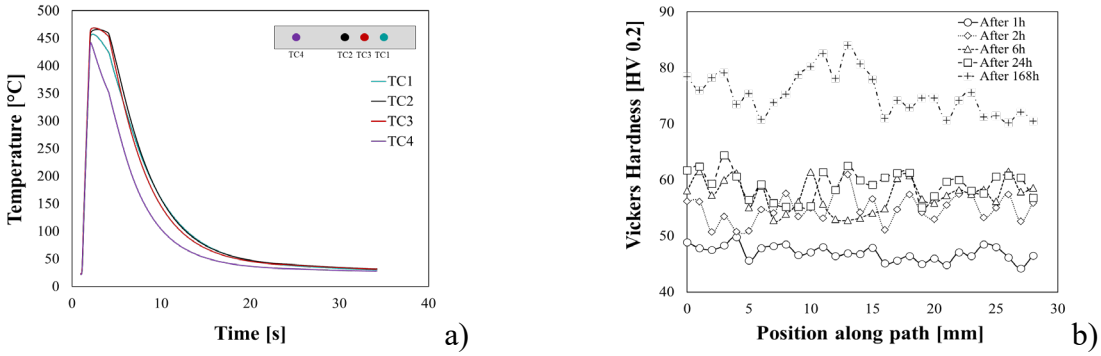

Figure 3 Results from the first Gleeble test (450°C for 2 s): (a) local temperature curves, (b) time evolution of the hardness values along the longitudinal path.

According to the results of the first tests, the subsequent ones were carried out at a lower temperature (350°C) and varying the soaking time over three levels (2. 5 and 10 seconds). As an example, the evolution of the hardness values of the specimen heat-treated setting the temperature to 350°C and the time to 5 s (see Figure 4a) suggested that the drop in the material hardness was remarkable (the reference value in the T6 condition is around 88 HV) and, above all, constant over time (up to one week), thus confirming the occurrence of the overaging.

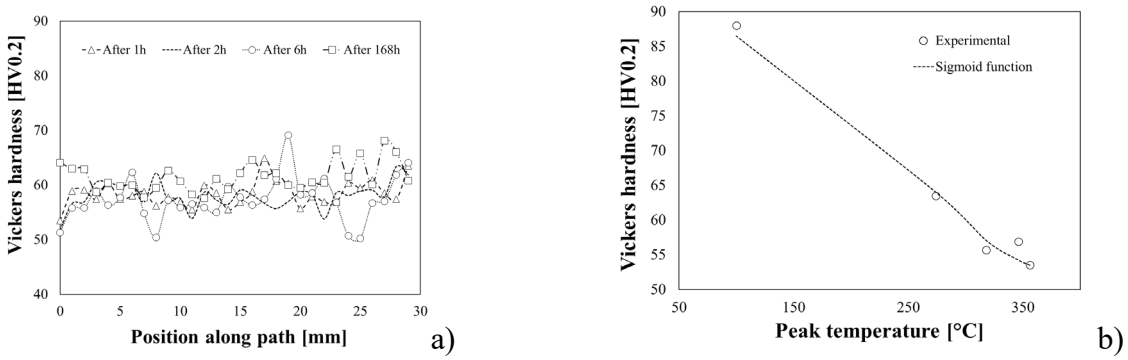

Figure 4 Results from Gleeble test at 350°C for 5 s: (a) time evolution of hardness along the measuring path, (b) the constructed sigmoid function

Similar results were obtained also in the other two tests setting different values of the holding time. The hardness measured close to the thermocouples could be then univocally related to the correspondent temperature. Measured values could be plotted as a function of the peak temperature reached during the heating test (corresponding to the temperature during the soaking step). Hardness values, as shown in Figure 4b, were fitted by a logistic function [12] whose analytical formulation is expressed by Equation 1.

$$HV = 88 - \frac{A}{1+\exp[\lambda(T_0-T_{max})]} \quad (1)$$

being A the maximum drop in the hardness (from the initial T6 state), T_0 the function's midpoint and λ the steepness of the curve. Nevertheless, an important aspect had to be assessed: the hardness measured at a specific location had not to be taken as the result of the only soaking step but had to be related to the whole thermal history (heating, soaking and cooling). Therefore, the integral below each extracted temperature/time curve (considered as an accurate indicator of the thermal history) was calculated and divided by the peak temperature reached during the test (i.e. the soaking temperature), thus obtaining the equivalent time (t^*). In such a way, the hardness value was considered to be determined by an equivalent heat treatment characterized by a constant

Materials Research Proceedings 35 (2023) 62-69 https://doi.org/10.21741/9781644902714-8

temperature (equal to the peak temperature) and a duration equal to t^*. Table 1 reports the calculated t^* values for all temperature curves; moreover, values referring to curves from the same Gleeble test (i.e. same soaking time) were then averaged (t^*_{avg}).

Table 1 List of extracted heating conditions along with the correspondent equivalent time

ID test	Peak Temp. [°C]	Soaking time [s]	t* [s]	t^*_{avg} [s]
T353-t2	353	2	7.26	6.99
T352-t2	352	2	7.09	
T329-t2	329	2	7.21	
T300-t2	300	2	6.39	
T351-t5	351	5	10.16	10.05
T345-t5	345	5	9.86	
T320-t5	320	5	10.34	
T274-t5	274	5	9.84	
T352-t10	352	10	14.69	15.50
T314-t10	314	10	15.51	
T256-t10	256	10	16.30	

Eventually, the hardness values from each Gleeble test were fitted by the sigmoid function, each related to a certain value of the average equivalent time. Therefore, the constants of the sigmoid (T_0 and λ) could be expressed as a linear function of the average equivalent time, as shown in Figure 5 (a and b).

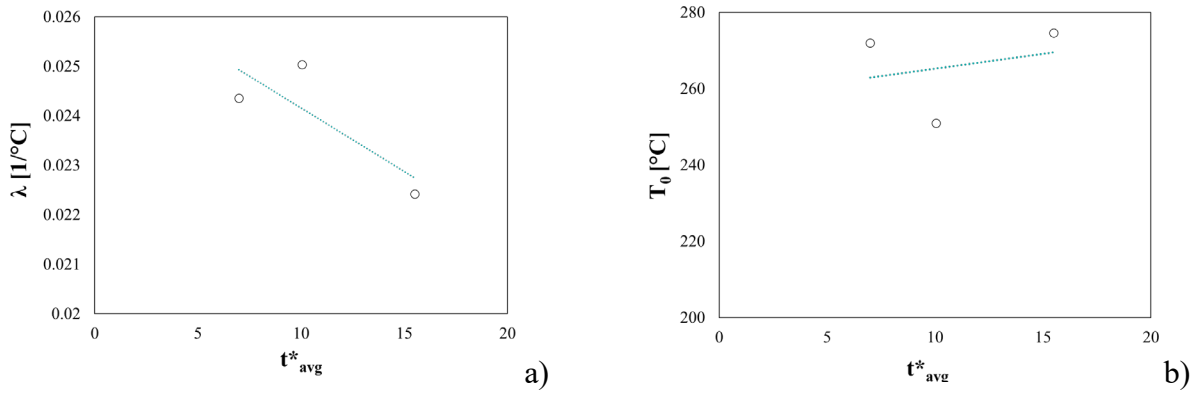

Figure 5 Constants of the logistic formulation as a function of t^*_{avg}: (a) λ and (b) T_0

Numerical results.

Preliminary FE simulations were run to calibrate the unknown thermal boundary conditions. Temperature acquired by the thermocouple (see Figure 2b) were used as target for tuning the FE model: differences between experimental data and the nodal temperature from the same location was minimized by setting the absorption coefficient to 0.49 and the convective heat transfer coefficient to 1 W/m^{2}K. The model could be thus used to simulate the effect of different values of the laser power and the holding time. Results in terms of temperature evolutions of the node positioned at the center of the laser spot have been plotted in Figure 6.

Materials Research Proceedings 35 (2023) 62-69 https://doi.org/10.21741/9781644902714-8

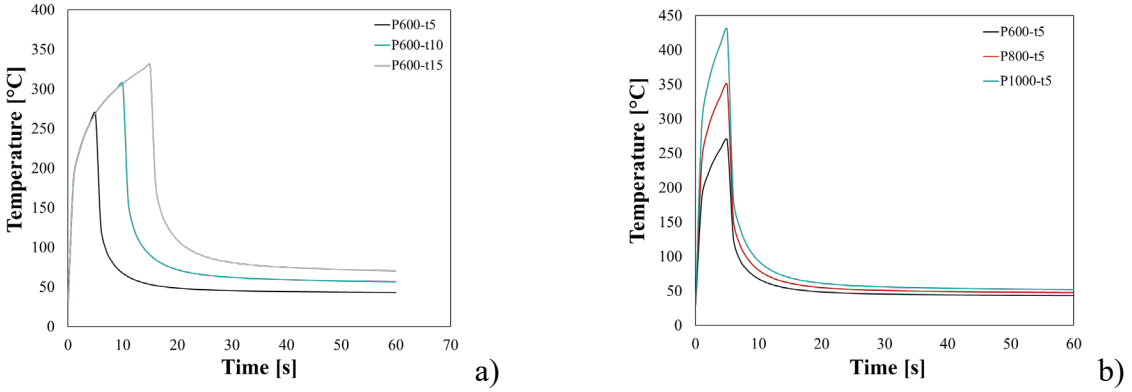

Figure 6 Simulation of the laser heating: (a) effect of the beam power, (b) effect of the heating time

Numerical results revealed a good accordance with the theory, since a remarkable increase in the peak temperature was reached when increasing the heating time (Figure 6a) or, alternatively, increasing the laser power (Figure 6b). For all the simulated conditions, the integral bounded by the temperature time curve extracted from the node located at the center of the spot was calculated and, once known the maximum temperature, the equivalent time was calculated. The equivalent time for all the simulated conditions have been reported in Table 2.

Table 2 Determination of the equivalent time for the investigated heating conditions

ID simulation	Laser power [W]	Heating time [s]	Max. Temp [°C]	Eq. time [s]
P600-t5	600	5	269.11	14.66
P600-t10	600	10	307.74	19.60
P600-t15	600	15	330.55	24.30
P800-t5	800	5	349.67	13.35
P800-t10	800	10	399.594	18.61
P800-t15	800	15	430.788	23.50
P1000-t5	1000	5	429.62	12.55
P1000-t10	1000	10	492.00	17.99
P1000-t15	1000	15	530.985	22.98

Post-processing of the numerical results. Starting from the numerical results of the laser heating, the final distribution of hardness was calculated by means of a Python script: the nodal temperature of each node was extracted by the script for all time instants, thus allowing to identify the peak temperature and to calculate the integral below the temperature-time curve. From the ratio between the integral and the peak temperature, the equivalent time could be calculated and the final hardness estimated using Equation 1. According to the results from the Gleeble tests at 450°C, heating simulations characterized by a nodal peak temperature close or higher then 400°C were not post-processed (presumably the treated region would have been brought to the fully solutioned state). Figure 7 shows the predicted final hardness distribution for the other post-processed conditions: only when setting the laser power at 800 W for 5 s, the drop in the material properties was much more pronounced and the predicted hardness in the heated zone below 60 HV.

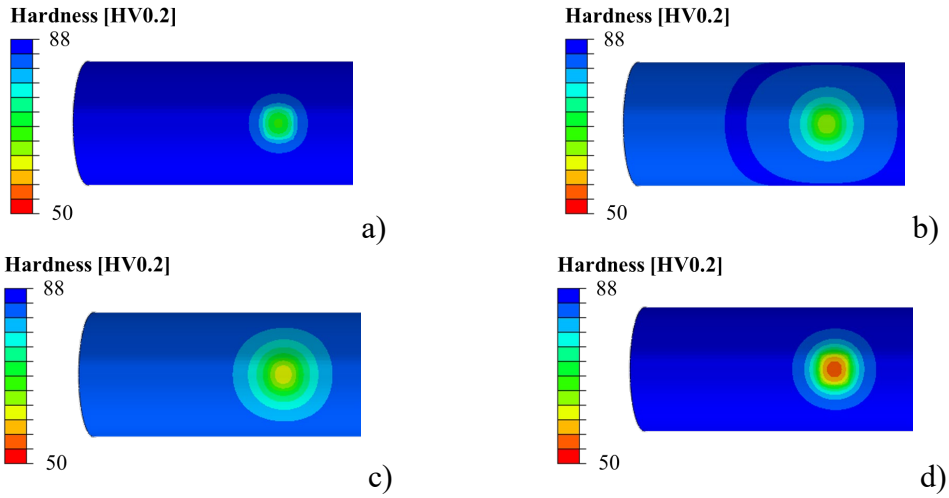

Figure 7 Numerical prediction of the final hardness distribution: (a) P600-t5, (b) P600-t10, (c) P600-t15, (d) P800-t5

Validation of the numerical predictions. According to the numerical results, the laser heating test conducted setting the laser power to 800 W and the heating time to 5 s was replicated. Once the tube cooled down to room temperature, the portion subjected to the laser heating was extracted and the hardness (in the thickness direction) monitored at different times. As reported in Figure 8, the hardness did not varied, thus revealing that overaged condition was reached. In addition, the measured values were in good accordance with the numerical prediction (continuous green line).

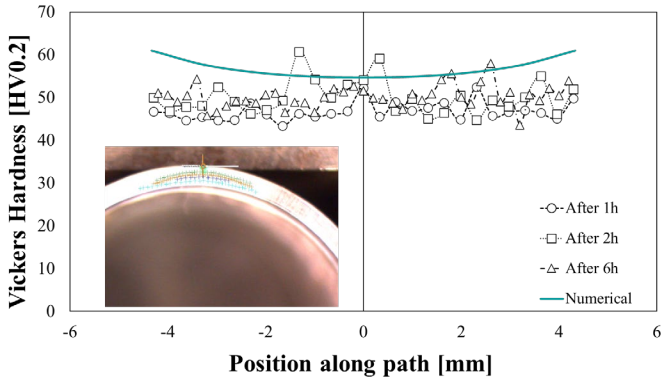

Figure 8 Experimental measured hardness vs. predicted values from the numerical simulations (P800-t5)

Conclusions

In the present work, an original methodology to predict the change of material properties determined by a laser heating on AA6063-T6 tubular parts has been proposed. The Gleeble physical simulator allowed to gather a large quantity of data by means of a limited number of tests. It was demonstrated that all the temperature close or above 400°C, even for very small holding time (few seconds), brought the material to the fully solutioned state; temperature of 350°C allowed to reach a more stable overaged condition. The preliminary characterization provided enough data to construct an analytical model: a sigmoid function was adopted to correlate the measured local hardness value to the peak temperature reached during the heating test. Moreover, in order to precisely correlate the final properties to the whole heat treatment (heating, soaking and cooling), measured hardness were also expressed as a function of the equivalent time t^*.The FE simulation of the tube laser heating, after having inversely calibrated the unknown thermal boundary conditions, allowed to discard all the combination of laser power and heating time that

led to a maximum temperature in the spot higher than 400°C in order to avoid the fully solutioning of the material (according to the results from the preliminary Gleeble tests at 450°C). Results from the FE simulations were post-processed by means of a Python script implementing the fitted sigmoid function: in such a way, it was possible to numerically predict the final hardness distribution. The experimental test reproducing the chosen heating condition (laser power equal to 800 W and heating time to 5 s) allowed to determine a good accordance between the numerical predicted hardness values and the experimental ones, thus confirming the effectiveness of the proposed approach. At the same time, future steps will be aimed at improving the model capability by enriching the characterization step using the Gleeble system: in particular, focusing the attention on a narrower range of temperatures around 400°C, it would be possible to evaluate the threshold condition discerning the overaged condition from the fully solutioned one. In such a way, any laser heating would ideally be designed according to the type of local modification to be achieved (fully solutioning rather than overageing).

References

[1] Mayer RM, Poulikakos LD, Lees AR, Heutschi K, Kalivoda MT, Soltic P. Reducing the environmental impact of road and rail vehicles. Environ Impact Assess Rev 2012;32:25-32. https://doi.org/10.1016/j.eiar.2011.02.001

[2] Hirsch J. Recent development in aluminium for automotive applications. Trans Nonferrous Met Soc China (English Ed 2014;24:1995-2002. https://doi.org/10.1016/S1003-6326(14)63305-7

[3] DIN EN 45545-2. Railway applications - Fire protection on railway vehicles - Part 2: Requirements for fire behaviour of materials and components 2016.

[4] Kalpakjian S, Schmid SR. Manufacturing processes for engineering materials. Singapore; London: Pearson Education; 2017.

[5] Geiger M, Merklein M, Vogt U. Aluminum tailored heat treated blanks. Prod Eng 2009;3:401-10. https://doi.org/10.1007/s11740-009-0179-8

[6] Piccininni A, Palumbo G. Design and optimization of the local laser treatment to improve the formability of age hardenable aluminium alloys. Materials (Basel) 2020;13. https://doi.org/10.3390/ma13071576

[7] Kahrimanidis A, Lechner M, Degner J, Wortberg D, Merklein M. Process design of aluminum tailor heat treated blanks. Materials (Basel) 2015;8:8524-38. https://doi.org/10.3390/ma8125476

[8] Peixinho N, Soares D, Vilarinho C, Pereira P, Dimas D. Experimental study of impact energy absorption in aluminium square tubes with thermal triggers. Mater Res 2012;15:323-32. https://doi.org/10.1590/S1516-14392012005000011

[9] Piccininni A, Magrinho JP, Silva MB, Palumbo G. Formability Analysis of a Local Heat-Treated Aluminium Alloy Thin-Walled Tube. Springer International Publishing; 2021. https://doi.org/10.1007/978-3-030-75381-8_230

[10] Buchanan K, Colas K, Ribis J, Lopez A, Garnier J. Analysis of the metastable precipitates in peak-hardness aged Al-Mg-Si(-Cu) alloys with differing Si contents. Acta Mater 2017;132:209-21. https://doi.org/10.1016/j.actamat.2017.04.037

[11] Sekhar AP, Nandy S, Ray KK, Das D. Prediction of Aging Kinetics and Yield Strength of 6063 Alloy. J Mater Eng Perform 2019;28:2764-78. https://doi.org/10.1007/s11665-019-04086-z

[12] Maalouf M. Logistic regression in data analysis: An overview. Int J Data Anal Tech Strateg 2011;3:281-99. https://doi.org/10.1504/IJDATS.2011.041335